TRANSIENT SIMULATION OF HARMONIC TEO CIRCUITS

Gregory B. Tait and Stephen H. Jones*

Electrical Engineering, Virginia Commonwealth University, Richmond, VA 23284
Email: gbtait@saturn.vcu.edu

*Dept. of Electrical Engineering, University of Virginia, Charlottesville, VA 22903

ABSTRACT

A fast, convolution-based computer algorithm is employed to simulate the fully autonomous operation of a complete millimeter-wave, harmonic transferred electron oscillator (TEO), and an investigation of harmonic power generation is presented. Unlike previous combined harmonic-balance/device simulations of oscillator circuits, the nonlinear physical device/circuit response evolves in time to its natural steady-state mode of operation which permits insights into harmonic energy exchange, stability, load pulling, and frequency tuning effects. A second-harmonic 150 GHz TEO is simulated using both conventional Gunn and novel stable-depletion-layer (SDL) InP devices. The SDL device prohibits the formation of accumulation layers and dipoles. The integrated device/circuit simulations in the time-domain enable us to investigate the formation and build-up of this stable mode in detail.

I. INTRODUCTION

At present, the lack of reliable, high-power, and compact solid-state sources is the single greatest obstacle to achieving an accessible submillimeter-wave technology. Advanced research is needed to create the next generation of THz sources suitable for scientific and commercial applications.

The role of device and circuit simulation is critical to understanding the operation of transferred-electron oscillators (TEO), frequency multipliers, and metal-semiconductor-metal (MSM) photomixers, and to designing a monolithic integrated circuit incorporating the complete THz circuit. In turn, only with fast, robust, and accurate numerical algorithms can computer-aided design (CAD) and analysis tools become practical to the design engineer. This work will help develop the necessary efficient and accurate computational algorithms to be used in future integrated device/circuit CAD.

Although harmonic-balance methods are successful in determining the steady-state behavior of millimeter-wave circuits, there are many important high-frequency and high-speed circuits that require full time-dependent simulation, including transients under discontinuous operating conditions (at start-up and other times) and

the mixing and parametric effects of multiple and possibly non-commensurate-frequency signals. The simulation of low-frequency nonlinear circuits is commonplace (e.g. SPICE simulations), but application of pure time-domain techniques to large-scale nonlinear microwave and millimeter-wave circuits is generally more complex [1]. In particular, any time-domain solution algorithm based on Newton-Raphson or optimization iterations of the nonlinear system virtually precludes the use of a physics-based numerical solid-state device simulator, since the necessary derivatives in the Jacobian matrix can not be practically generated from a purely numerical, "black-box" description of the nonlinear solid-state device.

Seminal work in convolution-based solution algorithms appeared in early literature[2], but has been largely neglected since that time, owing to unacceptably inefficient computer algorithms and lengthy compute times. Currently, with the wide-spread availability of high-speed workstations, interest in revisiting this approach has surfaced [3, 4]. However, efficient algorithmic implementation and applications to new devices and circuits have been lacking. Presently, a very large number of sample points in the discrete convolution, well over 10^5 , and time steps not exceeding a few femtoseconds need to be used. For a millimeter-wave oscillator circuit of moderate Q, it can take well over 10^6 time steps to reach a steady-state operation [3]. Another approach that allows steady-state operation to be reached much sooner requires the use of an additional time-integration scheme at each time step [4]. This is acceptable if the device can be modeled by an equivalent circuit, but highly undesirable if the device must be simulated by its physics-based numerical model. Clearly, a new approach is needed to improve computational speed, thus permitting the investigation and co-design of new devices and circuits.

II. Simulation Method

To meet the unique requirements of efficiency and accuracy in an integrated device/circuit simulator, an improved time-domain convolution-based algorithm must be developed. Specifically, the proposed new approach consists of applying advanced concepts from the fields of digital signal processing and nonlinear iteration theory to the discrete-time impulse response of the linear embedding circuit. The proposed solution method follows these steps:

1.) The complex, frequency-dependent embedding impedances as "seen" by each port of the solid-state device in its mount must be accurately determined. Care must be exercised in the sampling of the freqeuncy-domain impedances to insure sufficient resolution and to avoid unwanted aliasing effects in the associated time-domain impulse response. Complex embedding impedances of novel, state-of-the-art waveguide and coplanar mounts can be determined with the use of electromagnetic field simulators, such as the Hewlett-Packard High-Frequency Structure Simulator [5], a 3-D finite element code solving Maxwell's equations.

2.) The associated size of the discrete impulse response obtained from an inverse FFT of the complex impedance samples must be reduced by truncation if we are to achieve our goal of efficient simulation. Unfortunately, the nearly discontinuous structure of some embedding impedances (caused by waveguide cut-off and high-Q behavior) will lead to the familiar Gibbs-phenomenon ripples in the embedding impedance function that is reconstructed

from the discretized impulse response. Hence, both truncation and the Gibbs phenomenon will limit the accuracy of the derived impulse response. From the field of digital signal processing, finite-impulse-response digital filters can be designed to reshape the truncated impulse time samples in such a manner that ripples in the corresponding frequency-domain samples have been smoothed [6]. A large volume of literature has explored the optimal reshaping for the causal, linear-phase filters used in signal processing applications. It is unknown at the present time what kinds of reshaping functions will work best for impulse responses derived from the millimeter-wave circuits of interest. We can, however, create a whole new class of asymmetric filter, as we are only interested in maintaining the real, causal property of the impulse response (i.e., we are not constrained by linear-phase considerations). A new filter was used to generate the reshaped impulse response samples, retaining only 8000 terms from the original $2\text{x}10^5$. Figure 1 shows a comparison of the impedance samples reconstructed from the digitally filtered impulse response with the original embedding impedances of the model harmonic oscillator cavity.

3.) The discrete convolution used in the device/circuit solution algorithm is placed in an advantageous form suggested by the theory of nonlinear iteration:

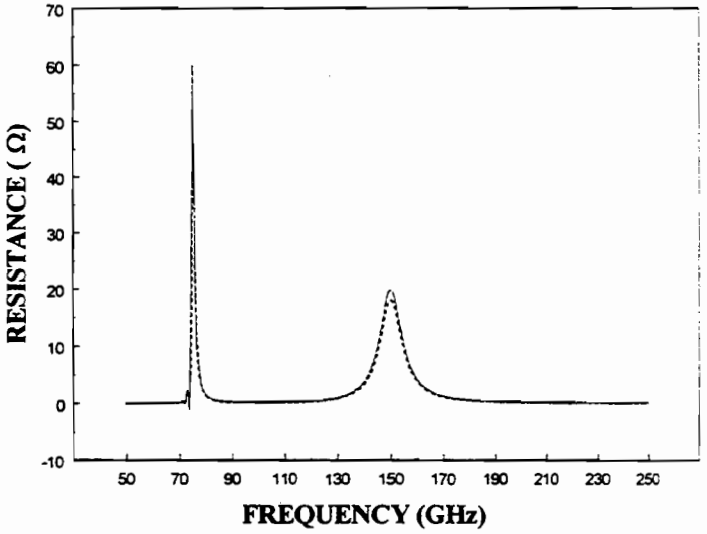

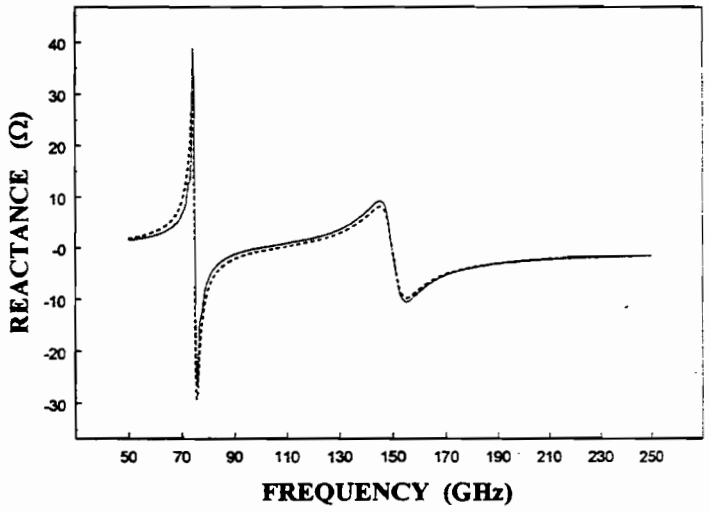

Figure 1. Reconstructed (solid line) and Original (dashed line) TEO Circuit Impedances

$$v_k = \sum_{j=k-N+1}^{k-1} h_{k-j} i_j(v_j) + h_0 i_k(v_k) \qquad (1)$$

where k indicates the time step level ($k\Delta t$) in the simulation, h_n are the impulse response samples, v and i are voltages and currents at the nonlinear device terminals. Equation (1) is in fixed-point iteration form.

If the time step Δt is very small, the "unknown" i_k can be approximated by $i_k \cong i_{k-1}$, and no iteration is needed. However, it may require well over 10^6 time steps until steady-state is achieved, and, at each step, the numerical solution to the device nonlinear differential equations and the convolution integral must be performed. The fixed-point iteration form, on the other hand, allows us to use the maximum-sized time step consistent with the stability and accuracy of the numerical device simulator. Although we may need to iterate on Eq. (1), as $i_k \cong i_{k-1}$ is not necessarily a good approximation, the under-relaxation and Steffensen acceleration schemes employed by us previously make the iteration subject to rapid convergence[7]. The semi-implicit time discretization scheme of our TED device simulator allows stable and accurate time steps such that steady-state oscillator operation is acquired after only 10^4 time steps, a savings in computational effort of two orders of magnitude. The combination of the very efficient convolution calculation performed at each time step with the reduced number of time steps necessary to reach steady-state operation leads to significant reduction in computer execution time.

4.) Since the summation term in the convolution, Eq.(1), contains all known values at time step k, it may be calculated in parallel with the solid-state device equations, yielding a further improvement in efficiency. We plan to implement the device/circuit solution algorithm in a massively parallel and distributed processing environment. Several high-performance UNIX workstations will collectively solve the complex device/circuit co-design problem.

A critical part of the success of the integrated device/circuit numerical approach is the efficiency and suitability of the physics-based numerical device simulator. The TED device used here is a modified version of a previously developed code [8]. The equations governing TED electron transport are the continuity equation, temperature dependent drift-diffusion equation, and Poisson's equation:

$$\frac{\partial n(x,t)}{\partial t} = \frac{1}{q}\frac{\partial J_n(x,t)}{\partial x} \tag{2}$$

$$J_n(x,t) = q\mu\left[\xi(x,t),T(x)\right]n(x,t)\xi(x,t) + qD\left[\xi(x,t),T(x)\right]\frac{\partial n(x,t)}{\partial x} + qn(x,t)D_T(x)\frac{\partial T(x)}{\partial x} \tag{3}$$

$$\text{and} \quad \frac{\partial^2 \psi}{\partial x^2} = \frac{q}{\varepsilon}\left[n(x,t) - N_D(x)\right] \tag{4}$$

where n, q, and J_n are electron density, electron charge, and electron particle current density, respectively. In Eq. (3), the field- and temperature-dependent mobility and diffusivity modeling parameters were extracted from three-valley Monte Carlo simulations. Lattice temperature in the device is calculated from a self-consistent solution to the heat equation for the packaged diode. These equations are discretized and solved using an accurate and efficient half-implicit Crank-Nicolson technique. Ohmic and fluid outflow boundary conditions are used at the cathode and anode of the device, respectively. The total device terminal current is given by:

$$I = \frac{A}{l}\int_0^l J_n dx + \frac{\varepsilon A}{l}\frac{dV}{dt} \qquad (5)$$

where A, l, and ε are the area, length, and material dielectric permittivity of the device. A fully self-consistent treatment of the displacement current term requires an accurate, second-order backward finite-difference calculation of the time derivative of terminal voltage in cases where a fully autonomous simulation is executed.

III. Simulation Results

Two circuits were simulated - one with a "conventional" notch-doped Gunn diode and one with a novel current-limiting-contact diode. Both devices have 1.8 μm InP active regions doped at 1 x 10^{16} cm^{-3} and are 60 μm in diameter. The Gunn diode has a 0.15-μm-long doping notch of 7 x 10^{15} cm^{-3} near the cathode. The current-limited diode has a shallow barrier (~110meV) cathode contact that prohibits the formation and propagation of accumulation layers and/or dipole domains. This device was experimentally developed by Litton Solid-State, and operates in a Stable Depletion Layer (SDL) mode characterized by the modulation of a stable depletion region [9]. Both diodes are inserted in a model second-harmonic, half-height WR-8 cavity. The embedding impedances presented to the diodes are modeled from representative data obtained from a combination of HP-HFSS and mode-matching simulations with equivalent circuit models. The transient simulations are shown in Figures 2 and 3.

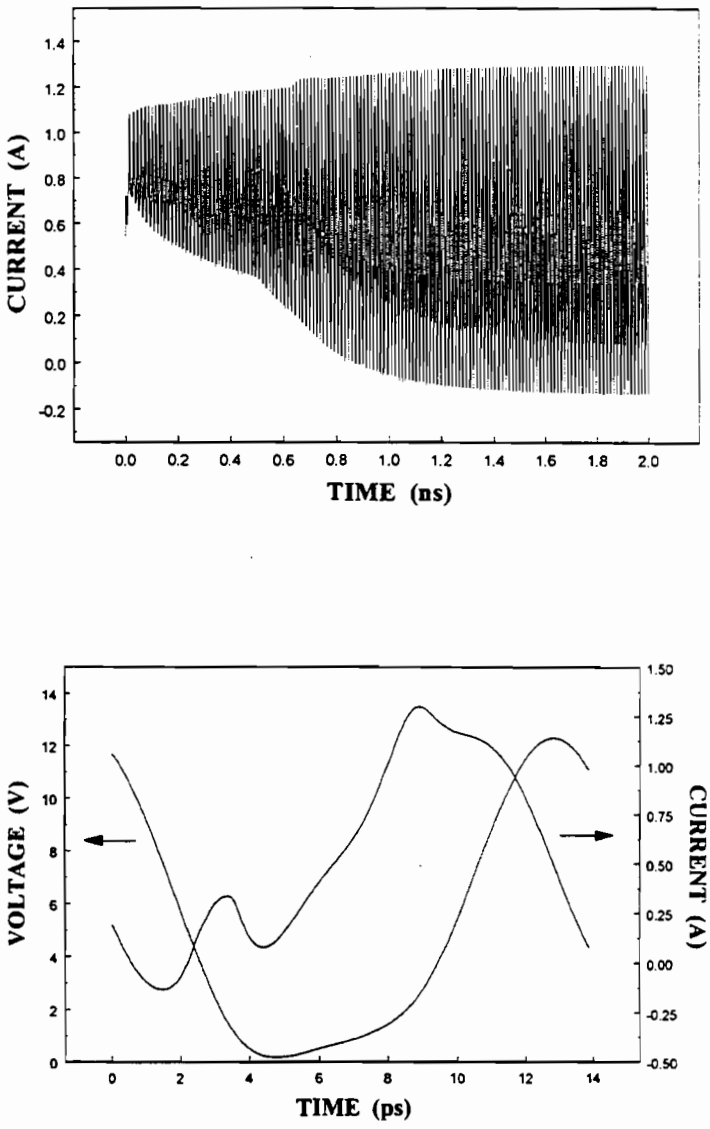

Figure 2. Transient and steady-state simulation of Gunn device terminal voltage and current in TEO circuit. Operating conditions are 5 VDC and 400 °K. Steady-state second-harmonic frequency settles at f_2 = 144 GHz.

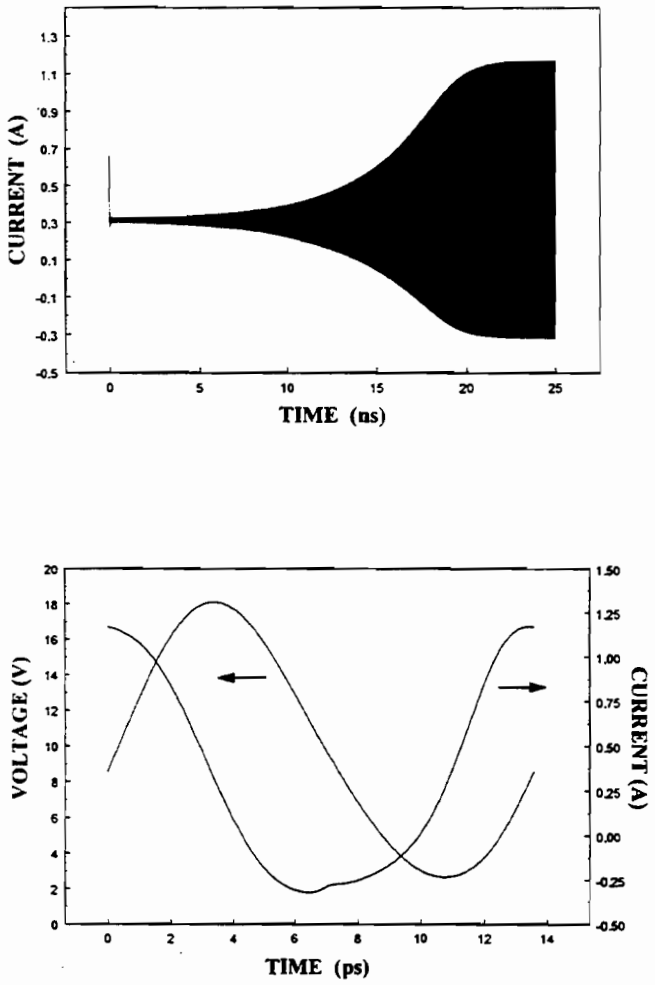

Figure 3. Transient and steady-state simulation of SDL device terminal voltage and current in TEO circuit. Operating conditions are 10 VDC and 400 °K. Steady-state second-harmonic frequency settles at $f_2 = 147$ GHz.

Both circuits exhibit a very large fundamental voltage oscillation near 73 GHz within the coaxial mount section of the cavity. The cut-off frequency of the output waveguide is at 75 GHz, so the diodes are terminated in a nearly pure reactance at the fundamental. Fourier analyses of the voltage and current waveforms show that very small amounts of power are actually dissipated at the fundamental frequency in the small series resistances of the diodes. In Fig. 2, we can actually see the rapid growth of the second harmonic current component, leading to considerable power generated at 144 GHz. A strong voltage oscillation at the fundamental frequency appears necessary to maintain this operation. We can understand this effect as energy conversion through the diode nonlinearity, much like the idler function in a frequency multiplier circuit. The second-harmonic is coupled to the output waveguide, while a backshort is adjusted to maximize output power. With proper design of the cavity dimensions, the real impedance seen at the second harmonic frequency is easily tuned to 1-20 Ω and the reactance is also tuned to 1-20 Ω. Since the fundamental frequency is in cut-off, impedance tuning at the second harmonic using the backshort should have little influence on the fundamental operation, with possible small parametric effects observed. Hence, a design is feasible with broad frequency tuning at the fundamental using a coaxial backshort and stable power tuning at the second harmonic using a waveguide backshort, with minimal coupled effects between the two tuners.

In Fig. 3, the transient solution for the SDL device indicates a much longer time to build-up a strong oscillation. Physically, the SDL device does not support strong unstable accumulation or dipole modes of operation, like the Gunn diode, but instead supports modulation of a steady electron density depletion. Through a combination of transferred electron effect, depletion layer transit time effect, and back-diffusion of carriers from the anode, the resultant asymmetric current waveform produces appreciable power generation at the second-harmonic. It may be possible to design for

increased harmonic content in the current waveform by tailoring the doping profile in the active region of the SDL device.

Table 1 demonstrates the effect of backshort tuning on the performance of the TEO circuit. A small diode series resistance (0.1 Ω) is included in the circuit impedances shown. The simulated output power at the second harmonic frequency compares well with experimental data [10]. In a WR-6 test cavity, output powers at a nominal 150 GHz ranged from 15-30 mW for several diodes in various package configurations.

IV. Conclusion

A time-domain technique has been developed that integrates numerical solid-state device simulation with complete nonlinear circuit simulation using an efficient convolution-based algorithm. This technique should aid in advancing the available CAD tools for submillimeter-wave components, especially harmonic TEOs, Schottky diode mixers, and MSM photomixers. Future developments will include implementation in a massively parallel and distributed computing environment, and the creation of Web-based CAD tools available to the THz community.

Backshort (degrees)	DC Power (W)	Z_1^{ckt} (Ω)	Z_2^{ckt} (Ω)	P_2 (mW)
+16	3.2	0.1 + j 10.0	7.7 - j 4.5	9.2
+6	3.2	0.1 + j 10.1	7.7 + j 3.6	18.0
+2	3.2	0.1 + j 10.2	3.7 + j 4.5	24.7
0	3.2	0.1 + j 10.2	3.1 + j 4.2	25.3
-2	3.2	0.1 + j 10.2	2.7 + j 4.0	25.1
-8	3.2	0.1 + j 10.1	1.5 + j 3.1	19.1
-14	3.2	0.1 + j 10.0	0.8 + j 2.3	10.9

Table 1. 147 GHz Second-Harmonic TEO Circuit Operation with 1.8 μm InP SDL Device

V. REFERENCES

1. R.J.Gilmore and M.B.Steer, "Nonlinear Circuit Analysis Using the Method of Harmonic Balance. A Review of the Art," *International Journal of Microwave and Millimeter-Wave Computer-Aided Engineering*, vol. 1, no. 1, pp. 22-37, Jan. 1991.
2. W.J.Evans and D.L.Scharfetter, "Characterization of Avalanche Diode TRAPATT Oscillators," *IEEE Trans. Electron Devices*, Vol. ED-17, No. 5, pp. 397-404, May 1970.
3. M. Curow, "New Insight in Operating Modes and Optimum Design of Harmonic TED Oscillators for W-Band Applications," *IEEE Trans. Electron Devices*, vol. 43, no. 6, pp. 861-870, June 1996.
4. M.B.Steer, "Oscillator Analysis," Workshop on Recent Advances in Microwave and Millimeter-Wave Oscillator Design, 1995 IEEE MTT-S International Microwave Symposium (Orlando, FL), May 16-20, 1995.
5. High-Frequency Structure Simulator, Release 5.0, Hewlett-Packard Company, Santa Rosa, CA, 1997.
6. A.V.Oppenheim and R.W.Schafer, *Discrete-Time Signal Processing.* Englewood Cliffs, NJ: Prentice-Hall Inc., 1989.
7. G.B.Tait, "Efficient Solution Method for Unified Nonlinear Microwave Circuit and Numerical Solid-State Device Simulation," *IEEE Microwave and Guided Wave Lett.*, vol. 4, no. 12, pp. 420-422, Dec. 1994.
8. G.B.Tait and C.M.Krowne, "Efficient Transferred Electron Device Simulation Method for Microwave and Millimeter-Wave CAD Applications," *Solid-State Electronics*, vol. 30, no.10, pp. 1025-1036, Oct. 1987.
9. M.F.Zybura, S.H.Jones, B.W.Lim, J.D.Crowley, and J.E.Carlstrom, "125-145 GHz Stable Depletion Layer Transferred Electron Oscillators," *Solid-State Electronics*, vol. 39, no. 4, pp. 547-553, April 1996.
10. M.F. Zybura, *A Theoretical and Experimental Contribution to the Design of 100-200 GHz Transferred Electron Oscillators.* Ph.D. Dissertation, University of Virginia, Jan. 1996.